Extension of the Bonn meson exchange NN potential above pion production threshold: Role of the delta isobar

Ch. Elster,* K. Holinde,† and D. Schütte
Institut für Theoretische Kernphysik, Universität Bonn, Nussallee 14-16, D-5300 Bonn, Federal Republic of Germany

R. Machleidt
Los Alamos National Laboratory, Los Alamos, New Mexico 87545 and Department of Physics, University of California, Los Angeles, California 90024
(Received 19 November 1987)

Based on a meson exchange NN interaction, which contains $N\Delta$ and $\Delta\Delta$ box diagrams, the contributions of one-pion loop self-energy corrections to the nucleon and delta-isobar propagators are studied. In the framework of time-ordered perturbation theory, their independent iteration on both baryon lines leads to dressing factors which give well-defined off-shell corrections to the meson exchange contributions and provide the isobar width. Results are presented for the NN phase shifts and a number of observables up to 1 GeV. Satisfactory agreement with empirical data is found, indicating no need for introduction of genuine quark effects.

I. INTRODUCTION

Although quantum chromodynamics (QCD) is believed to be the theory of strong interactions in terms of the fundamental constituents, i.e., quarks and gluons, conventional hadrons like nucleons, delta isobars, and mesons surely remain the relevant (collective) degrees of freedom for a wide range of low-energy nuclear physics phenomena. Hadron masses, coupling constants, and vertex form factors, which are the physical parameters of such a theory, are then left to be ultimately explained by QCD. Moreover, in the large N_c limit (N_c being the number of colors), QCD is supposedly equivalent to a local meson field theory. In any case, meson exchange is at present, and in the foreseeable future, the only quantitative model for the nucleon-nucleon (NN) interaction. Such a representation of the nuclear force, provided by an underlying physical picture, is needed as a starting point for a consistent description of the large field of nuclear structure physics including the important subtleties due to mesonic and isobar degrees of freedom.

Recently,[1] the Bonn group has presented a meson-exchange model of the NN interaction for application below pion production threshold. It is solely based on meson-nucleon-nucleon and meson-nucleon-delta-isobar (Δ) vertices W_α, which represent a natural and effective description of complicated multiquark reactions. W_α contain form factors F_α, which suppress the meson-exchange contributions for high momentum transfers, i.e., small distances. The presence of such form factors is dictated by the extended quark structure of the hadrons. In lack of a reliable determination from QCD, they are parametrized in the conventional monopole form with a parameter Λ_α, the so-called cutoff mass, which is determined empirically by a fit to the two-nucleon data.

The vertices W_α build up an infinite number of (irreducible) meson-exchange processes contributing to the NN interaction V. (Reducible diagrams are generated by the scattering equation.) In practice, however, one should make a choice according to the following guidelines: First, since the total meson mass exchanged between two nucleons determines the range of the NN force (higher mass implying shorter range), one should restrict oneself to meson exchanges with a mass below the cutoff mass Λ_α. The reason is that it does not make sense to take meson exchange seriously in a region in which modifications due to the extended structure are applied. With $\Lambda_\alpha \sim 1.3$ GeV, it is, therefore, reasonable and consistent to include all relevant exchanges up to a mass of about 1 GeV.

Furthermore, not only uncorrelated but also correlated 2π-exchange processes should be considered since there is a strong interaction between two pions. In fact, this correlated 2π-exchange contribution provides about $\frac{2}{3}$ of the total 2π exchange.

In addition, one has to take into account the structure of π and ρ exchange; namely, the corresponding tensor forces have opposite sign. Thus, there is partial cancellation between explicit 2π-exchange diagrams and those involving $\pi\rho$ exchange. Consequently, it is imperative to group them together.

There are further 3π-exchange contributions of comparable range, which, however, due to a similar counterstructure between correlated $\pi\pi$ S-wave contributions (providing attraction) and (repulsive) ω exchange, are to a large extent cancelled by corresponding 4π-exchange terms. In fact, those cancellations become even stronger in higher orders. In this way, convergence in our diagrammatic expansion is clearly established provided that the diagrams are grouped in a suitable way as dictated by the physics of the NN problem. This convergence is further improved (a) by the presence of form factors, and (b) due to the empirically established repulsive core of the NN interaction. Both phenomena reduce to the influence of higher-order short-ranged contributions.

Based on this (full) Bonn model (see Ref. 1), a quantitative description of the deuteron data, NN scattering phase shifts, and observables below pion production threshold in achieved. Most noticeably, the resulting tensor force is quite weak, which is seen in a low percentage D state of the deuteron, whereas the quadrupole moment and the asymptotic D/S state of the deuteron are large and in perfect agreement with experiment. The weak tensor force can be attributed to ρ exchange, a realistic πNN form factor, and the inclusion of meson retardation.

There are several reasons for this thorough and comprehensive approach to the NN interaction. First, there is a rather basic motivation: One wants to know if, and to what extent, meson exchange alone is able to provide a quantitative model for the NN interaction. Obviously, the extremely good reproduction of the empirical NN data with this model proves the usefulness of the meson-exchange picture as an effective description of the (low-energy) NN interaction. Furthermore, the field-theoretical approach provides an unambiguously defined off-shell behavior of the nuclear force. Moreover, the vertex functions (with parameters being fixed) together with the set of diagrams contributing to the NN interaction form a sound basis for a well-defined and consistent generalization to three-body forces and meson-exchange-current contributions to the electromagnetic properties of nuclei.

Naturally, the next step is to extend the model of Ref. 1 above the threshold of pion production, i.e., above a nucleon lab energy of about 300 MeV. The interest in this (inelastic) region was stimulated by a series of polarized beam experiments which showed a strong energy and polarization dependence of various observables at intermediate energies. Phase shift analyses[2,3] showed counterclockwise looping in the Argand diagrams for several partial waves and suggested an interpretation in terms of genuine dibaryon resonances. However, since pion production provides strong inelasticities in this energy region, the counterclockwise looping may also be caused by the opening of isobar channels, mainly the N-Δ channel, which can be handled in the conventional framework.

In order to really decide whether meson exchange remains a valid concept above pion threshold, i.e., up to a nucleon lab energy of about 1 GeV, the same vertices, fixed below threshold, should now be used consistently, both in the elastic and inelastic channels, or in other words, in the NN interaction and in the pion production mechanism. However, the energy dependence of the (time-ordered) meson propagators leads to direct meson production. (Note that the use of static propagators does not include this possibility.) Therefore, in order to still guarantee unitarity, nucleon and delta-isobar self-energy diagrams (which, so far, have only roughly been taken into account by using empirical masses, see Ref. 1) must now be included explicitly.

In a first step[4] (referred to as I in the following) we have studied self-energy effects arising from the dressing of the nucleon. This step is relatively simple since it can be treated on the one-boson-exchange (OBE) level. Nevertheless, it has sufficient structure to provide insight into the characteristic features and problems encountered in renormalization. We have demonstrated that, in the framework of noncovariant perturbation theory, the independent iteration of one-pion loops on both nucleon lines leads to dressing factors which provide well-defined off-shell corrections to the meson-exchange contributions. It turned out that nucleon dressing yields additional attraction in lower partial waves. A slight readjustment of meson parameters (especially a reduction of the cutoff mass in the πNN vertex) leads to a reproduction of the empirical NN data below pion threshold which is of the same quality as before. The resulting inelasticities are, however, much too small. Therefore a different mechanism is needed which couples to the NN system to pionic channels. The most obvious way to do this is to let pion production proceed via virtual delta-isobar intermediate states. These are of outstanding importance already below pion threshold since they provide about half of the intermediate-range attraction of the nuclear force (see Ref. 1). So, for several reasons, there is compelling need for the inclusion of such contributions, which is the subject of the present paper.

In Sec. II, we will define the model and describe the basic formalism of including isobar self-energy effects. Section III provides the results, which consist mainly of NN phase shifts and some observables up to 1 GeV. Some concluding remarks are given in Sec. IV.

II. FORMALISM

A. Definition of the model

The starting point of our considerations is the Bonn meson-exchange NN interaction (see Ref. 1), which contains iterative as well as noniterative (stretched and crossed box) diagrams. Although the latter contributions proved to be quite important for a quantitative fit of the data below threshold they have not been included explicitly in the present work since their evaluation (including self-energy effects) is extremely involved. Their contribution is roughly taken into account by appropriately raising the correlated 2π S-wave contribution, which is, in the Bonn potential, effectively described by a scalar isoscalar σ exchange. Note however that such a procedure suppresses contributions to inelastic channels. Consequently, our present approach will certainly underestimate them. Nevertheless, the iterative diagrams, which we include, should provide the dominant contribution to pion production.

Thus, our model for the potential consists of the following diagrams, which are unitarized in the scattering equation:

(i) One-boson-exchange diagrams (π,ω,δ) and the correlated 2π exchange in P wave (ρ) and S wave (σ).

(ii) Iterative box diagrams involving $N\Delta$- and $\Delta\Delta$-intermediate states with $\pi\pi$, $\pi\rho$, and $\rho\rho$ exchange (Fig. 1).

Note that in order to fulfill the weak unitarity bound $(\sigma_{\text{tot}} > \sigma_{\text{el}})$ diagrams with double-ρ exchange, which are not present in the Bonn potential,[1] must be included now. For their explicit evaluation, we refer the reader to Refs. 1 and 5.

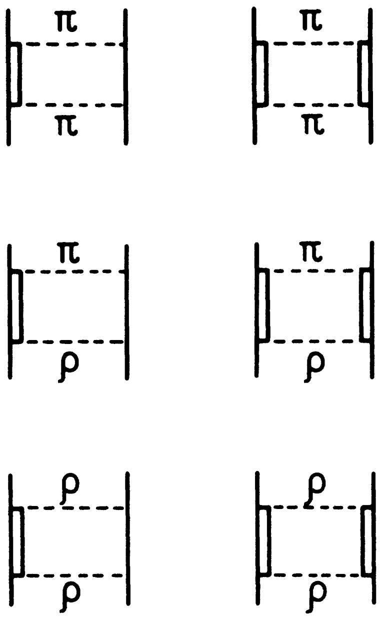

FIG. 1. $N\Delta$- and $\Delta\Delta$-box diagrams contained in the present model.

B. Isobar box diagrams including self-energy effects

Above pion threshold, the singularity structure of the diagrams in Fig. 1 gets more complicated: In the considered energy range up to 1 GeV, singularities appear in those propagators of the transition potentials $V_{N\Delta}$ and $V_{\Delta\Delta}$ which involve a pion. They are very similar to those of the one-pion-exchange (OPE) interaction between two nucleons. In fact, the region in which the singularities of the transition potentials are located, has the same bounds as the region of the singularities of the OPE propagator. So we can use the same (complex) contour deformation technique for solving the scattering equation as used in I.

Let us now turn to the effects resulting from the dressing of the Δ isobar. As for the nucleon [Fig. 2(a)], we restrict ourselves to the simple (Lee-model-type) self-energy diagram involving the pion only [Fig. 2(b)]. It has been shown in I that, in time-ordered perturbation theory, the independent iteration of the bubble diagram, Fig. 2(a), on both nucleon lines leads to off-shell corrections, contained in a (multiplicative) dressing factor to the meson exchange diagrams. For example, the iterative diagram involving dressed NN intermediate states now acquires the following structure

$$\sum_{\alpha_1\alpha_2} V^{NN}_{\alpha_1''\alpha_2''\alpha_1\alpha_2}(z)\frac{1}{{}_{NN}R^{-2}_{\alpha_1\alpha_2}(z)(z-E_{\alpha_1}-E_{\alpha_2})}V^{NN}_{\alpha_1\alpha_2\alpha_1'\alpha_2'}(z) , \tag{2.1}$$

where $V^{NN}(z)$ is the conventional (energy-dependent) OBE-interaction containing renormalized quantities only. z is the starting energy and the sum goes over the intermediate states α_1,α_2. The characteristic dressing factor ${}_{NN}R^{-2}_{\alpha_1\alpha_2}(z)$ depends, as expected, on the starting enegy and the intermediate states; it is given explicitly in I.

A corresponding factor ${}_{N\Delta}R^{-2}_{\alpha_1\alpha_2}(z)$, generated by the dressing of the nucleon as well as of the Δ isobar, arises in $N\Delta$ box diagrams. Furthermore, since the Δ is a resonant state, its energy gets an imaginary part which is related to the resonance width. Therefore, the inclusion of such self-energy effects leads to the following structure of $N\Delta$ box diagrams

$$\sum_{\alpha_1\alpha_2} V^{N\Delta}_{\alpha_1''\alpha_2''\alpha_1\alpha_2}(z)\frac{1}{{}_{N\Delta}R^{-2}_{\alpha_1\alpha_2}(z)\{z-[E^{\Delta}_{\alpha_1}-i\Delta_{\alpha_1}(z-E_{\alpha_2})]-E_{\alpha_2}\}}V^{N\Delta}_{\alpha_1\alpha_2\alpha_1'\alpha_2'}(z) . \tag{2.2}$$

Here $V^{N\Delta}$ is the interaction describing the transition $NN\to N\Delta$.

The argument of Δ_{α_1} takes into account that the imaginary part of the Δ self energy depends on the presence of the spectator nucleon α_2. According to Appendix A, it can be written as

$$\Delta_{\alpha_1}(z-E_{\alpha_2})={}_{N\Delta}R^{2}_{\alpha_1\alpha_2}(z)\tilde{h}^{\Delta}_{\alpha_1}(z-E_{\alpha_2}) , \tag{2.3}$$

where

$$\tilde{h}^{\Delta}_{\alpha_1}(z-E_{\alpha_2})\equiv\pi\sum_{\beta k}|W^{(\Delta N\pi)}_{\alpha_1\beta k}|^2\delta(z-E_{\alpha_2}-E_\beta-\omega_k) \tag{2.4}$$

is the imaginary part of the delta bubble diagram [Fig. 2(b)] with $W^{(\Delta N\pi)}_{\alpha_1\beta k}$ denoting the $\pi N\Delta$ vertex function. Analogously to the NN case, see I, the dressing factor can be written as

$$\begin{aligned}{}_{N\Delta}R^{-2}_{\alpha_1\alpha_2}(z)=1-(z-E^{\Delta}_{\alpha_1}-E_{\alpha_2})[\Gamma^{\Delta}_{\alpha_1}(z-E_{\alpha_2})\\ +\Gamma_{\alpha_2}(z-E^{\Delta}_{\alpha_1})]\end{aligned} \tag{2.5}$$

with

$$\Gamma^{\Delta}_{\alpha_1}(z-E_{\alpha_2})=\sum_{\beta k}\frac{|W^{(\Delta N\pi)}_{\alpha_1\beta k}|^2}{(E^{\Delta}_{\alpha_1}-E_\beta-\omega^{\pi}_k)^2(z-E_{\alpha_2}-E_\beta-\omega^{\pi}_k)} \tag{2.6}$$

for the dressing of the delta isobar and

$$\Gamma_{\alpha_2}(z-E^{\Delta}_{\alpha_1})=\sum_{\beta k}\frac{|W^{(NN\pi)}_{\alpha_2\beta k}|^2}{(E_{\alpha_2}-E_\beta-\omega^{\pi}_k)^2(z-E^{\Delta}_{\alpha_1}-E_\beta-\omega^{\pi}_k)} \tag{2.7}$$

for the dressing of the nucleon. ($E^{\Delta}_{\alpha_1}$ is the relativistic energy of the Δ isobar.)

The generalization to $\Delta\Delta$ box diagrams can be done in a straightforward way. Their structure is given by

$$\sum_{\alpha_1\alpha_2} V^{\Delta\Delta}_{\alpha_1''\alpha_2''\alpha_1\alpha_2}(z) \frac{1}{{}_{\Delta\Delta}R^{-2}_{\alpha_1\alpha_2}(z)\{z-[E^{\Delta}_{\alpha_1}-i\Delta_{\alpha_1}(z-E_{\alpha_2})]-[E^{\Delta}_{\alpha_2}-i\Delta_{\alpha_2}(z-E_{\alpha_1})]\}} V^{\Delta\Delta}_{\alpha_1\alpha_2\alpha_1'\alpha_2'}(z) , \tag{2.8}$$

where

$$\Delta_{\alpha_i}(z-E_{\alpha_j}) = {}_{\Delta\Delta}R^{2}_{\alpha_1\alpha_2}\tilde{h}^{\Delta}_{\alpha_i}(z-E_{\alpha_j}) \tag{2.9}$$

and

$$\begin{aligned} {}_{\Delta\Delta}R^{-2}_{\alpha_1\alpha_2}(z) &= 1-(z-E^{\Delta}_{\alpha_1}-E^{\Delta}_{\alpha_2}) \\ &\quad \times[\Gamma^{\Delta}_{\alpha_1}(z-E^{\Delta}_{\alpha_2})+\Gamma^{\Delta}_{\alpha_2}(z-E^{\Delta}_{\alpha_1})] . \end{aligned} \tag{2.10}$$

III. RESULTS AND DISCUSSION

The meson parameters of our model used throughout this paper are given in Table I. Note that the inclusion of self-energy corrections leads to a constraint for the pion cutoff since the Z factor, which characterizes the norm of the nucleon and Δ state, respectively (see I) must remain positive. This condition implies an upper limit of $\Lambda_{NN\pi}$ in the range of 1200 MeV if a monopole form factor at the vertex is used and leads to $Z_q^{-2}(m)=0.36$ (which means that the total nucleon wave function consists of a 64% pion cloud). A roughly equivalent choice, which is used here, is a dipole form with $\Lambda_{NN\pi}=1700$ MeV leading to $Z_q^{-2}(m)=0.44$ fm for the nucleon together with a mass shift $Z_q^{-2}(m)h_q(m)=-585$ MeV.

Based on the quark model value $f^2_{N\Delta\pi}/4\pi=0.224$, a corresponding limit of $\Lambda_{N\Delta\pi}=1000$ MeV is obtained for the Δ isobar, which yields $Z_q^{-2,\Delta}(m_\Delta)=0.62$ and a resonance shift $Z_q^{-2,\Delta}(m_\Delta)h_q^{\Delta}(m_\Delta)=-517$ MeV.

Figure 3 shows the momentum dependence of the Z factor. (A corresponding result is obtained for the mass shift.) Obviously, it stays essentially the same in the relevant momentum range, i.e., the amount of pion cloud does not depend on the momentum of the particle, which is physically appealing.

We next want to study the effect of baryon dressing on the $N\Delta$ box diagram $W(q',q\ 2E_{q_0})$ [Eqs. (2.2)]. Figure 4 shows the contribution of W in the ${}^1S_0$ state, for $q'=q_0=250$ MeV, as function of q. (Note that $\pi\pi,\pi\rho$ as well as $\rho\rho$ exchange is included.) Like in the NN case (see I), the $N\Delta$ dressing factor ${}_{N\Delta}R_q^{-2}(z)$ enhances the (attractive) contribution of the $N\Delta$ interaction. Furthermore, the dressing of the nucleon gives an effect about twice as large as the dressing of the Δ isobar. Consequently, delta dressing in diagrams with $\Delta\Delta$ intermediate states is comparably unimportant. Since baryon dressing is an off-shell effect it is quite small in higher partial waves. However, in lower partial waves, it has a visible effect leading always to additional attraction, especially for higher energies. This is due to the fact that here the iterations of the potential become important, which are attractive and are increased by the dressing factor. In our model, this additional attraction is compensated for by the use of slightly stronger cutoffs than used in Ref. 1.

Above pion production threshold the contribution of the $N\Delta$ box diagrams becomes complex, firstly due to the delta width, which appears in the box propagator [see Eq. (2.2)], secondly because of singularities present in the $N\Delta$ dressing factor as well as in the pion exchange propagators. It turns out that the main contribution to the imaginary part of the interaction and therefore to the inelasticities is given by the delta width. The contributions of the pion propagators are of the same magnitude as those in the NN case (see I) and thus quite small.

The quantity characterizing the Δ width, $\tilde{h}^{\Delta}_q(z-E_q)$ depends on the starting energy z as well as on the momentum q of the (intermediate) Δ state. As Fig. 5 demonstrates, this dependence is quite dramatic: $\tilde{h}^{\Delta}_q$ grows with increasing z, but drops off quite fast for higher momenta q. (The dependence on the spin state λ is negligibly small.)

We mention that the contribution of box diagrams involving $\Delta\Delta$ intermediate states is quite small, because of the higher threshold.

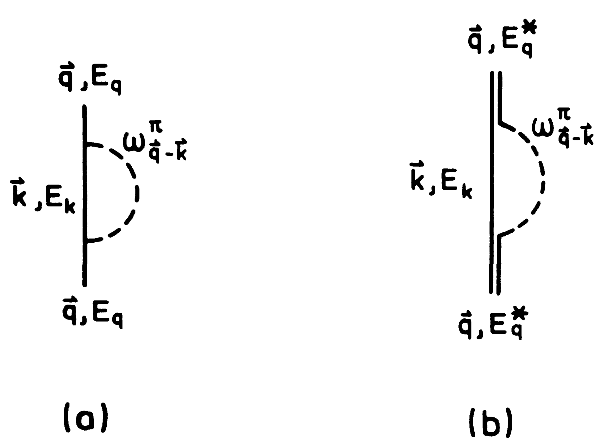

FIG. 2. Nucleon (a) and delta isobar (b) self-energy diagram involving the pion.

TABLE I. Meson parameters used in the present model. The form factors at the vertices are parametrized as $F_\alpha \equiv (\Lambda_\alpha^2 - m_\alpha^2/\Lambda_\alpha^2 + (\mathbf{q}-\mathbf{k})^2)^{n_\alpha}$.

	$\frac{g_\alpha^2}{4\pi}$	m_α (MeV)	Λ_α (MeV)	n_α
$NN\pi$	14.4	138.03	1700	2
ρ	0.7(6.1)	769.0	1400	1
ω	20.0	782.6	1650	1
σ	8.8396	580.0	1600	1
δ	0.0567	983.0	2000	1
	$\frac{f_\alpha^2}{4\pi}$	m_α (MeV)	Λ_α (MeV)	n_α
$N\Delta\pi$	0.224	138.03	1000	1
$N\Delta\rho$	15.51	769.0	1500	2

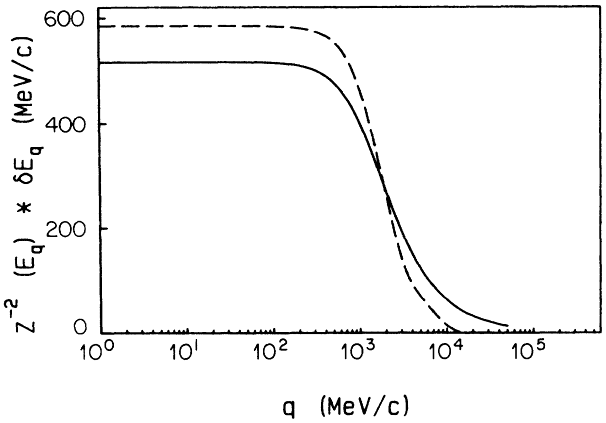

FIG. 3. Z-factor of the nucleon [$Z_q^{-2}(E_q)$; dashed line] and of the delta isobar [$Z_q^{-2,\Delta}(E_q^{\Delta})$; solid line] as function of the particle momentum q.

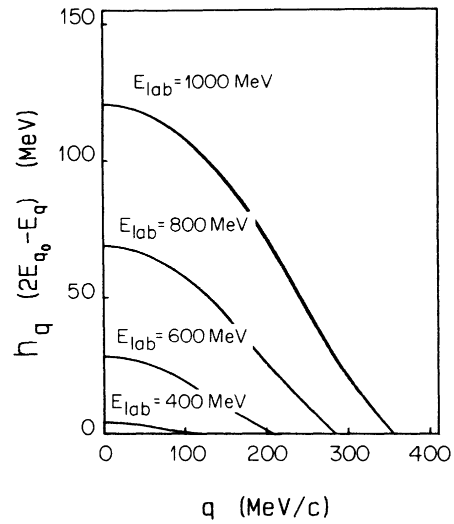

FIG. 5. Delta width for various starting energies z as function of the particle momentum q. $z \equiv 2E_{q_0}$ is related to the lab energy $E_{\rm lab} = 2q_0^2/m$.

The partial wave phase shifts and inelasticity parameters, obtained from our model by solving a Lippmann-Schwinger equation for the scattering amplitude T, are shown in Fig. 6 for isospin 1 and compared to results from empirical analyses. Obviously, the latter differ widely from each other, especially for the inelasticity parameters, which is an indication that experimental data still contain rather large uncertainties in the energy region above pion production threshold.

We also did a calculation with a q-independent Δ width, putting $q=0$ in $\tilde{h}_q^{\Delta}(z-E_q)$ but keeping the starting-energy dependence. As expected from Fig. 5, such a procedure overestimates the inelastic contributions especially in the energy region shortly above pion production threshold. This is in line with results obtained already by Kloet and Tjon.[7] The differences between these two off-shell extrapolations of the delta width are most clearly seen in the higher partial waves $^1G_4$ and $^3F_4$. In the $^3F_4$ state, the constant delta width overestimates the correct result in the whole energy region, whereas in the $^1G_4$ state it overestimates the correct result for energies smaller than 700 MeV and underestimates it for larger energies. Here both calculations lie in between the empirical analyses, whereas in the Argand plot of the $^1G_4$ state (see Fig. 7) only the calculation with the q- and z-dependent delta width lies close to the experimental points. The constant delta width shows a more resonancelike behavior because of its stronger looping.

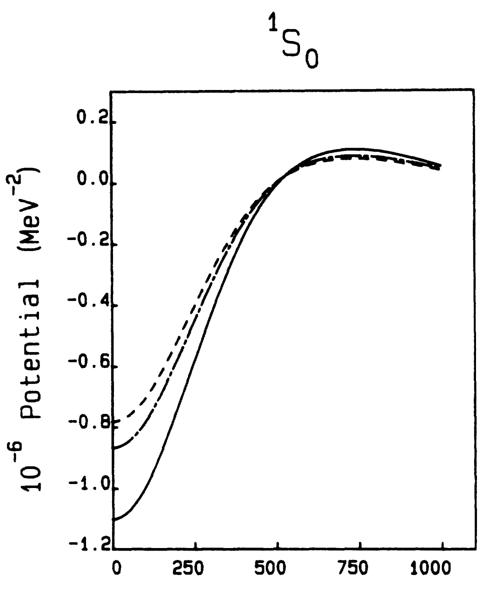

FIG. 4. Effect of the dressing factor ${}_{N\Delta}R_q^{-2}(z)$ on the $N\Delta$-box diagram, $W(q',q\,|\,2E_{q_0})$ [Eq. (2.2)], for $q'=q_0=250$ MeV. The dashed line shows W without any baryon dressing. The dash-dot line is obtained by dressing the Δ isobar, the solid line contains delta as well as nucleon dressing.

The most interesting partial wave states of the $T=1$ channels are the $^1D_2$ and $^3F_3$ states because in both states the NN-$N\Delta$ threshold is very important. Both partial waves are very inelastic and show a counterclockwise looping in the Argand plot with increasing energy, see Fig. 8. Note that for $^3F_3$ the looping is not strong enough compared to the empirical data. Obviously, the inelastic threshold provided by our model is not strong enough, which is not surprising since, e.g., we left out the inelasticities arising from crossed-box diagrams.

The effect of the individual contributions to the NN interaction for these two states is displayed in Figs. 9 and 10. They both show a strong bump when the attractive $N\Delta\pi\pi$ contribution is added. Especially in the $^1D_2$ state, this strong attraction is suppressed by adding the short-range repulsion given by $\pi\rho$ exchange.

The NN partial wave phase shifts for the $I=0$ channels are displayed in Fig. 11. Apart from the $^1P_1$ state the empirical data are described fairly well. The inelasticities are solely arising from conventional one-pion exchange and thus quite small; see I.

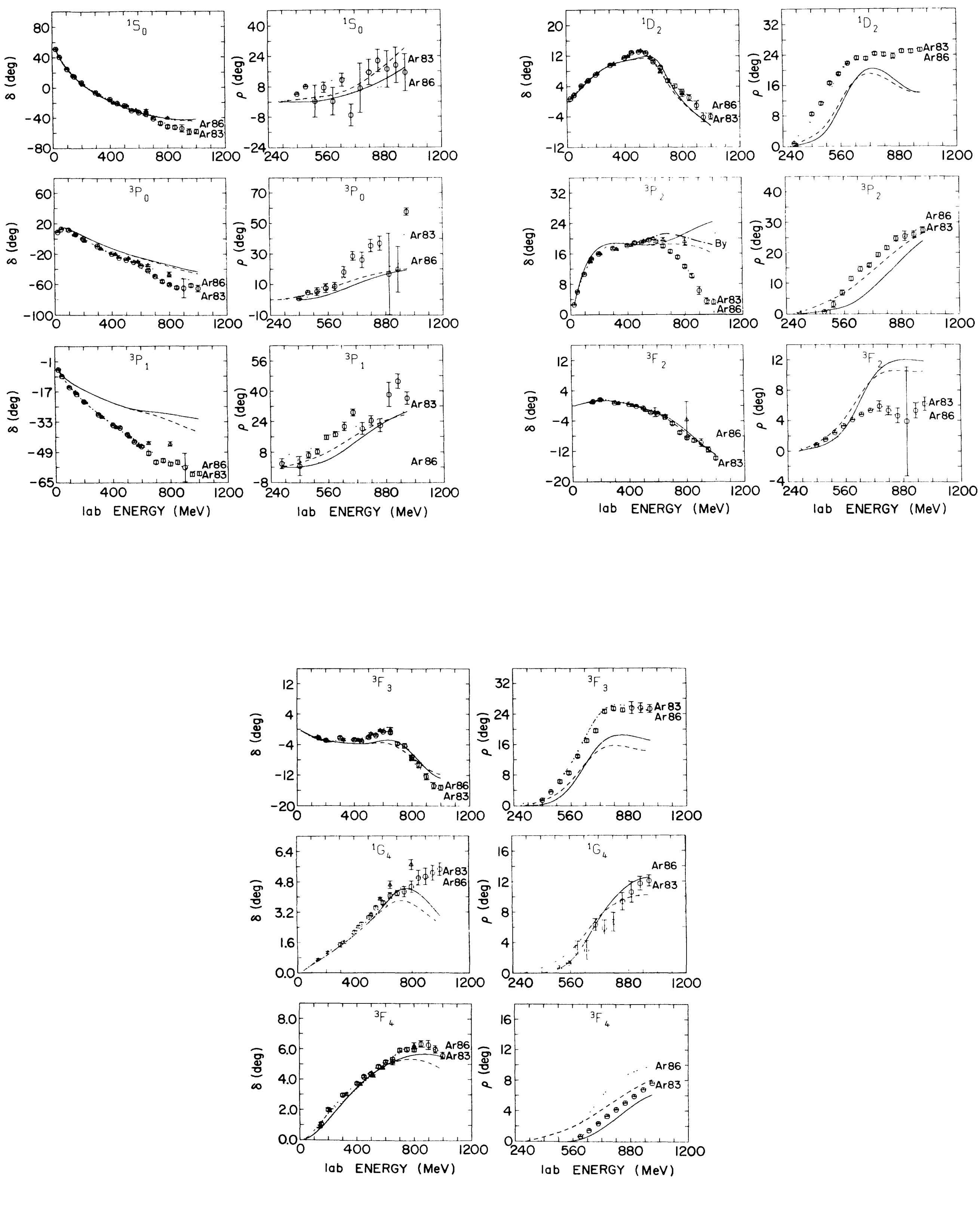

FIG. 6. Isospin-1 phase shifts obtained from the present model (solid line). The dashed line results from a calculation with a q-independent delta width. The error bars are taken from Ref. 2 (octagon) and Ref. 3 (triangle). The dotted (Refs. 2 and 6) and dash-dot (Refs. 26 and 27) lines show different empirical analyses.

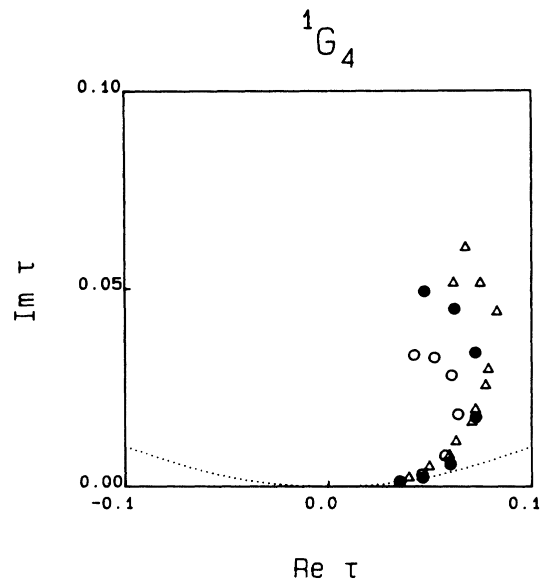

FIG. 7. Argand plot of the partial wave phase shift $^1G_4$ in NN scattering. The result of the present model for lab energies from 400 MeV to 1000 MeV is given by solid circles whereas open circles stand for a calculation with a q-independent delta width. The experimental data points (open triangles) are taken from Ref. 7, the dotted line represents the unit circle.

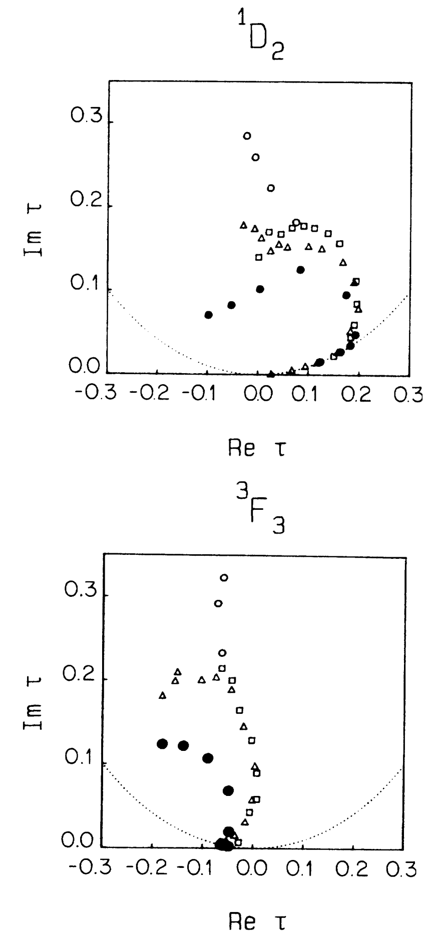

FIG. 8. Argand plots of the partial wave phase shifts $^1D_2$ (a) and $^3F_3$ (b) in NN scattering. Solid circles denote the results of the present model for lab energies from 200 MeV to 1000 MeV. The experimental data points are taken from Ref. 6 (open triangles), Ref. 26 (open squares), and Ref. 27 (open circles); the dotted line represents the unit circle.

It should be noted that the discrepancies between the different empirical analyses are here even more pronounced than in the $T=1$ channels. Especially for the inelasticities the data seem to be quite uncertain and should be improved. This would be of special importance if $N\Delta$-crossed-box diagrams will be included since these also contribute to $I=0$ states.

We now want to compare the results of our model to those obtained by Faassen and Tjon,[8] who work in a covariant Bethe-Salpeter framework. The physical content of their model is however comparable. The authors likewise leave out crossed-box diagrams and neglect (virtual) antiparticle contributions; they automatically keep stretched-box diagrams, which are however quite small. Therefore it should be of no surprise that their results are very similar compared with ours. For example, their inelasticities in $^1D_2$ and $^3F_3$ are also too small. Note that the model of Ref. 8 contains $N\Delta$-ΔN transitions, which we leave out in order to avoid a coupled channel formalism. Therefore, the unitarity is not exactly fulfilled in our model whereas the weaker unitarity condition $\sigma_{\text{tot}} > \sigma_{\text{el}}$ still holds. Since the numerical results are so similar for both models these transitions obviously play only a minor role in the NN channel.

So far in this work we have always compared the predictions of our model above pion production threshold with empirical phase shift analyses. As discussed before, these still contain uncertainties, especially for the inelasticities. Therefore, we have also computed several scattering observables for which experimental data exist. For the calculations we have used partial waves up to $J=25$, neglecting the (negligible) contributions of the $N\Delta$- and $\Delta\Delta$-diagrams for $J > 10$.

We first turn our attention to the inelastic cross section due to single-pion production, see Fig. 12. (The results in Figs. 12–16 have been derived from the optical theorem. This is only approximately correct since, in the present stage, our model is not exactly unitary. The expected minor changes should not affect our qualitative conclusions.) Our model as well as that of Ref. 8 underestimates the empirical data considerably. This was to be expected since the inelasticity parameters of the strongly inelastic partial wave amplitudes are undersized, too. As mentioned before, the reason is that processes providing further inelasticity are still missing in both models.

Note that the use of a momentum-independent delta width, which overestimates the inelastic contributions, can in fact provide a rougly correct description of the empirical data. However, as discussed before, it leads to inconsistencies in the partial wave inelasticity parameters.

The inelastic longitudinal cross section difference $\Delta\sigma_L^{\text{in}} := \Delta\sigma_L^{\text{in}}(\rightleftarrows) - \Delta\sigma_L^{\text{in}}(\rightarrow)$ is a sensitive measure of the balance (or imbalance) of the pseudoresonant channels $^1D_2$ and $^3F_3$ since the contributions of singlet and uncoupled triplet waves enter with positive, respectively, negative sign. Moreover, the inelastic cross sections are independent of the phase shifts and therefore only sensitive to the pion production rate.

The wrong description of $\Delta\sigma_L^{\mathrm{in}}$ given by the meson exchange model of Kloet and Silbar,[10] see Fig. 13, is sometimes taken as a proof for the necessary failure of conventional meson theory in general. However, this model is based on a $N\Delta$ interaction with pion exchange only, which is known to overestimate the $^1D_2$ state considerably. In our model, $\pi\rho$-exchange together with retardation effects in the meson propagators puts the balance in the right direction.

An even better balance is obtained from a calculation by Jauch, König, and Kroll.[11] These authors start with a deck model for the *NN* interaction, in which the isobar production amplitude is given by single π exchange with the πN amplitude taken from empirical data. This pure deck model describes the data as poorly as the model of Ref. 10. If then the contribution in the $^3F_3$ state is artificially enhanced by adding a phenomenological piece assumed to arise from a 3^--dibaryon state, the data are described quite well (though not perfectly). However, we strongly feel that it is premature to consider this as an unambiguous signal for a genuine dibaryon resonance, since already in the present stage our model provides a reasonable description and there is still considerable room for improvement in the conventional meson exchange framework.

In Fig. 14, we compare our results for the inelastic transverse cross section difference, $\Delta\sigma_T^{\mathrm{in}}$, with the results obtained in Refs. 8 and 10. Again, as expected, the unrealistic (due to lack of $\pi\rho$ exchange) meson exchange model of Ref. 10 strongly overestimates the data. Note that this cannot be cured by adding again a corresponding 3^--dibaryon since now uncoupled triplet states do not contribute. Thus a consistent description of both $\Delta\sigma_L^{\mathrm{in}}$ and $\Delta\sigma_T^{\mathrm{in}}$ seems to be possible only if conventional $\pi\rho$ exchange is included.

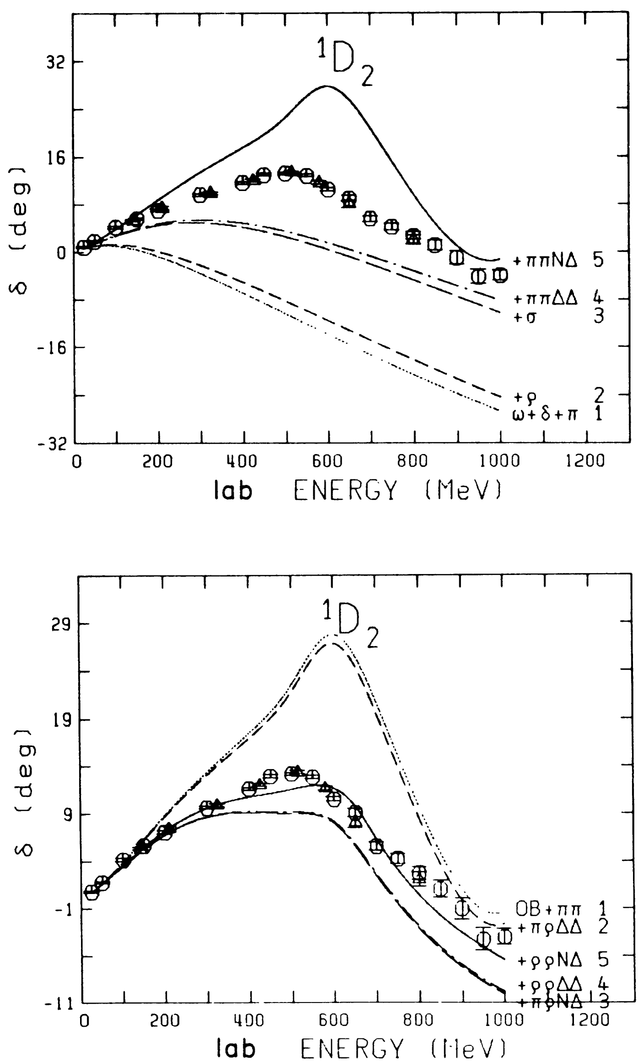

FIG. 9. $^1D_2$ phase shift of *NN* scattering. The effects of the individual contributions to the *NN* interaction are displayed: (a) shows the one-boson and 2π-exchange contributions, (b) those of $\pi\rho$ and $\rho\rho$ exchange. They are added up successively in the order given on the right-hand side of the curve labels.

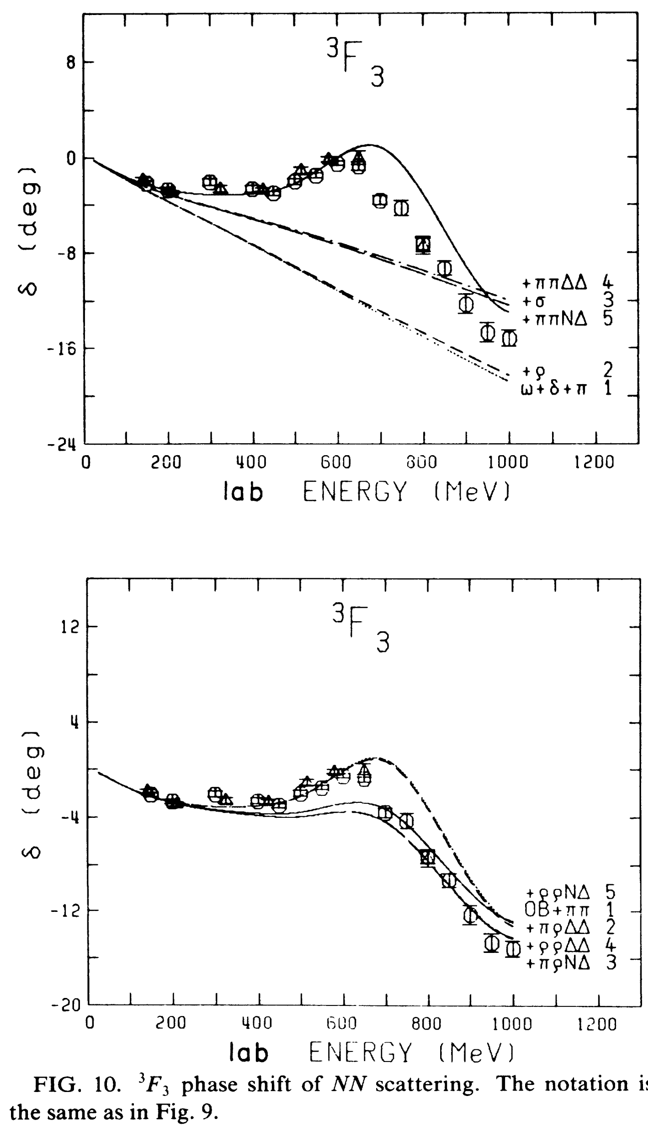

FIG. 10. $^3F_3$ phase shift of *NN* scattering. The notation is the same as in Fig. 9.

The corresponding total cross section differences $\Delta\sigma_T$ and $\Delta\sigma_L$ are shown in Figs. 15 and 16. The predictions for $\Delta\sigma_T$ of our model have the right shape and the right order of magnitude; only their energy dependence is slightly wrong. On the other hand, $\Delta\sigma_L$ is seriously overestimated. (A comparable result has been obtained in Ref. 8.) The reason is that now the real phase shifts enter, which are not described sufficiently accurately by the present model. Of course, if the $\pi N\Delta$ -vertex providing the pion production mechanism is treated independently from that in the NN interaction and $NN \rightarrow N\Delta$ transition potential by using e.g., different cutoff parameters, a better description can easily be obtained.[17,18] However, it should be clear that such a procedure, although possibly connecting a sizable amount of data, is surely not able to really explore the range of validity of the meson exchange picture.

In this connection we would like to make some remarks concerning the relation of our model to πN scattering, especially in the P_{33} partial wave. In the simplest, Lee-model-type approach (see Appendix A) the P_{33} amplitude is built up by iterations of bubble diagrams involving the Δ isobar, Fig. 2(b). With the parameters for the $\pi N\Delta$ vertex used in our NN model (see Table I), we calculated the imaginary part of the P_{33} scattering amplitude. As shown in Fig. 17, the resulting resonance width is much too narrow compared to the empirical data, and it is well known that, in this framework, much smaller cutoff masses are required. Indeed, with $f^2_{N\Delta\pi}/4\pi=0.36$ and $\Lambda_{N\Delta\pi}=300$ MeV, a reasonable description is ob-

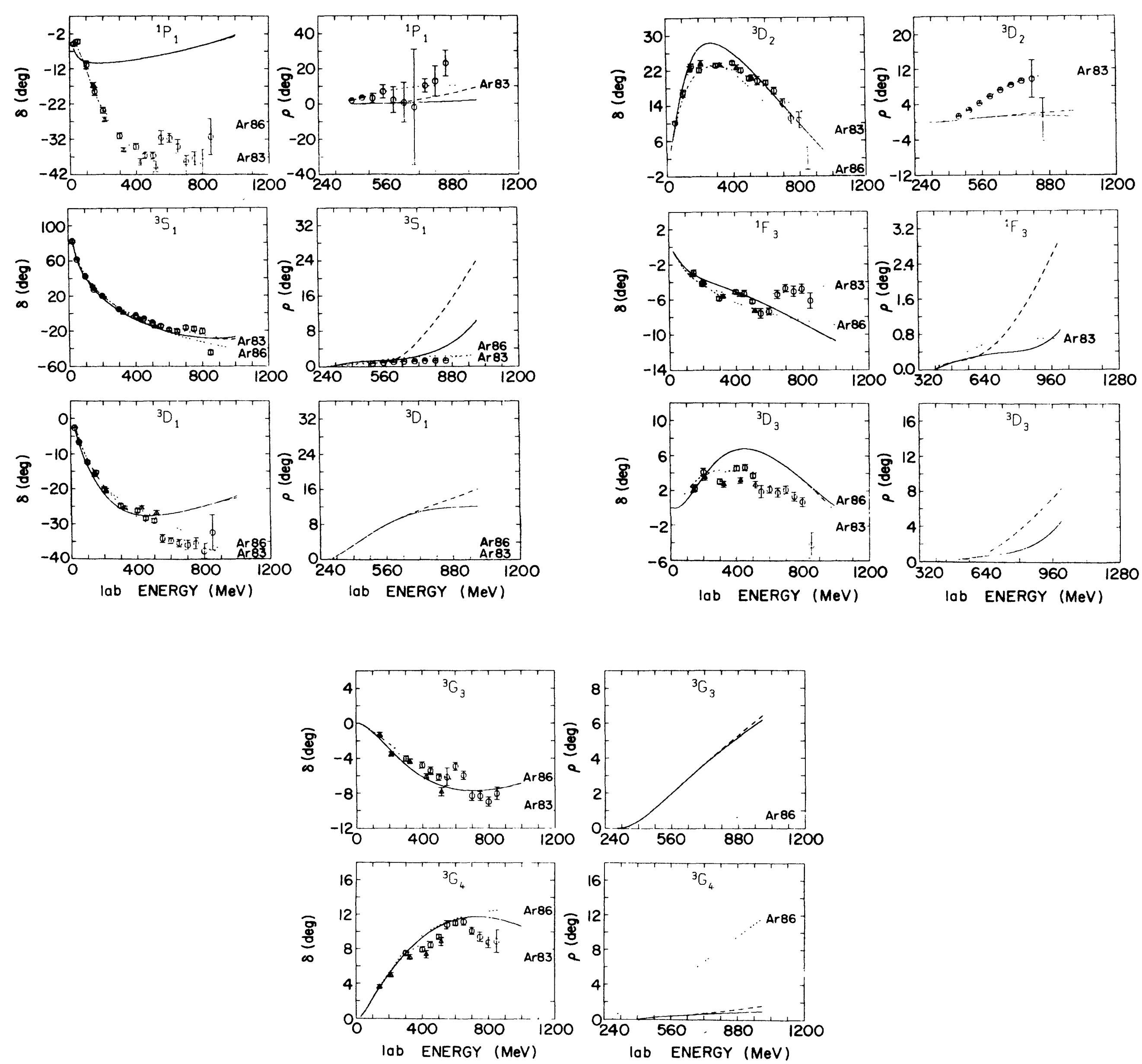

FIG. 11. Isospin-0 phase shifts for the present model (solid line). The notation is the same as in Fig. 6.

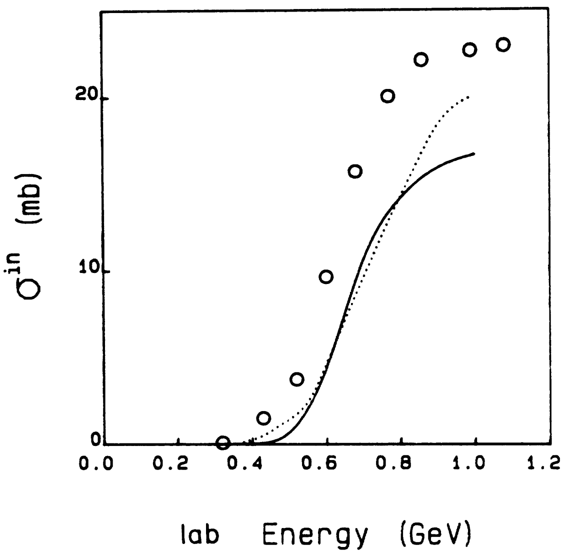

FIG. 12. Inelastic cross section due to single-pion production. The prediction of our model is represented by the solid line. The dotted curve results from a similar calculation taken from Ref. 8. The experimental data are taken from Ref. 9.

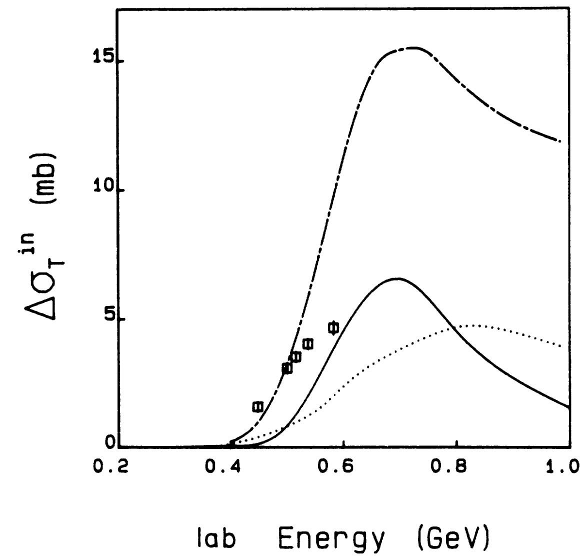

FIG. 14. Inelastic transverse cross section difference $\Delta\sigma_T^{\text{in}}(pp \rightarrow NN\pi)$. The prediction of our model (solid line) is compared with the results of Ref. 10 (dash-dot line) and with those obtained in Ref. 8 (dotted line). The experimental data points are taken from Ref. 13.

tained. We stress, however, that it is absolutely impossible to use such parameters consistently in our *NN* potential model. Because of the extremely small cutoff mass, the diagrams involving Δ isobars would give almost no contribution to the *NN* interaction and consequently the resonance structure in the *NN* channels would disappear completely. Thus, one might be tempted to conclude that a consistent and simultaneous description of the *NN* and πN system is not possible in the meson-exchange framework. This conclusion is however much too hasty; namely, we have to realize that the Lee-model-type approach used for πN is much too simple. A consistent treatment clearly requires to include further diagrams; especially the nucleon crossed graph gives a sizable contribution. In fact, it has been shown[20] that the inclusion of such diagrams, with parameters consistent with those of *NN* scattering, strongly improves the agreement with the empirical situation.

If one nevertheless wants to describe the *NN* and πN interaction (in the P_{33} partial wave) simultaneously by using for the latter system only the Lee-model-type pole

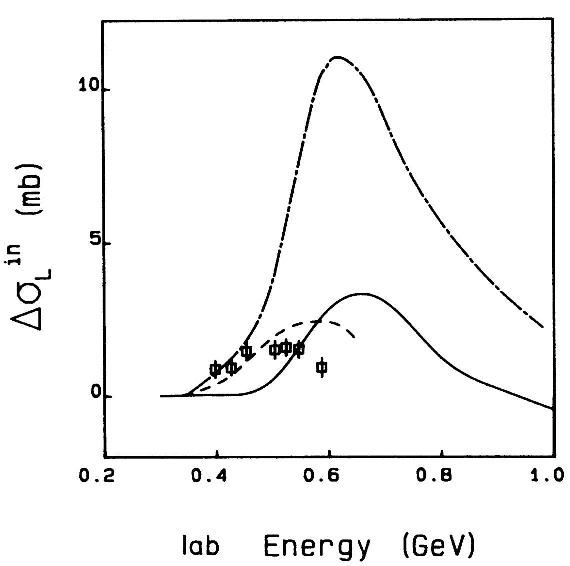

FIG. 13. Inelastic longitudinal cross section difference $\Delta\sigma_L^{\text{in}}(pp \rightarrow NN\pi)$. The prediction of our model (solid line) is compared with the results of Ref. 10 (dash-dot line) and Ref. 11 (dashed line). The experimental data are taken from Ref. 12 and do not include πd contributions.

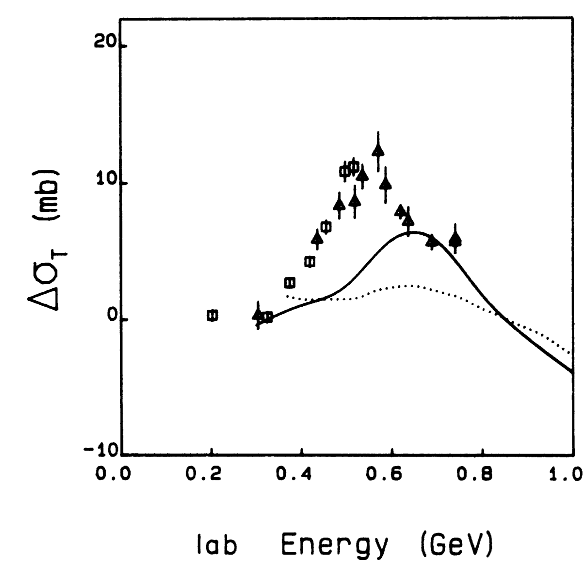

FIG. 15. Transverse cross section difference $\Delta\sigma_T$. The prediction of our model (solid line) is compared with that of Ref. 8 (dotted line). The experimental data points are taken from Ref. 14 (open squares) and Ref. 6 (open triangles).

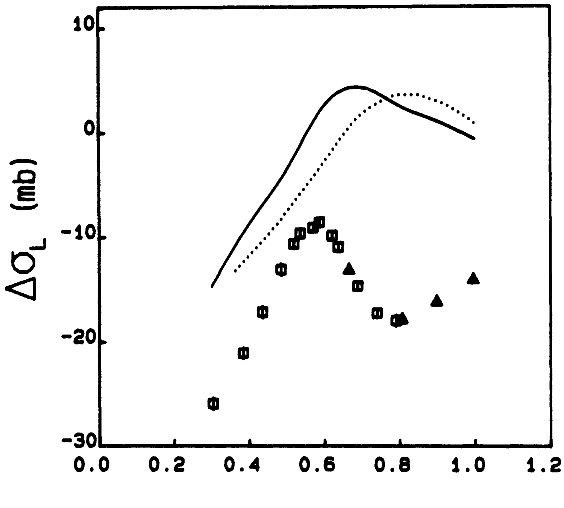

FIG. 16. Longitudinal cross section difference $\Delta\sigma_L$. The notation is the same as in Fig. 15. The experimental data points are taken from Ref. 15 (open squares) and Ref. 16 (open triangles).

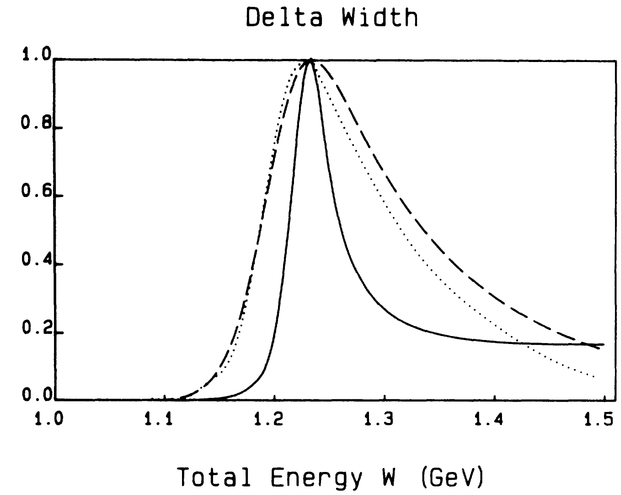

FIG. 17. Imaginary part of the πN T matrix in the P_{33} partial wave plotted vs the total energy of the πN system. The solid line shows a Lee-model-type calculation with $f^2_{N\Delta\pi}/4\pi=0.224$ and $\Lambda_{N\Delta\pi}=1000$ MeV whereas the dashed curve is obtained with $f^2_{N\Delta\pi}/4\pi=0.36$ and $\Lambda_{N\Delta\pi}=300$ MeV. The experimental curve (dotted line) is taken from Ref. 19.

graph, one has to use completely different parameter values in the $\pi N\Delta$ vertex appearing in the transition potentials and in the isobar self-energy diagram. In order to test whether such a parameter choice has a sizable effect on the NN partial wave phase shifts we left the parameters of the exchange contributions unchanged but used for the delta bubble diagram $f^2_{N\Delta\pi}/4\pi=0.36$ and $\Lambda_{N\Delta\pi}=300$ MeV. Such an inconsistent treatment only slightly enhances the bump structure in $^1D_2$ and $^3F_3$ as well as their inelastic contribution for higher energies, but leaves the other partial wave phase shifts essentially unaltered. As discussed before, major effects on the NN inelasticity parameters arise from the special off-shell extrapolation of the isobar width.

In Table II the predictions of our model for the deuteron data and the low-energy scattering parameters are given and compared with the experimental values. Obviously, the characteristic features of the model presented in Ref. 1, namely a small D-state probability of the deuteron combined with a quadrupole moment Q_D which is rather large and reasonably close to the experimental value is not affected by the one-pion loop self-energy con-

TABLE II. Deuteron and low-energy scattering parameters predicted by the present model.

	Theory	Experiment
	Deuteron	
Binding energy ε_d (MeV)	2.22461	2.224575±0.000009[c]
D-state probability P_D (%)	4.67	5.0±2.0[a]
Quadrupole moment Q_D (fm^2)	0.282	0.2860±0.0015[d]
Asymptotic S state A_S (fm$^{-1/2}$)	0.8927	0.8846±0.0016[b,e]
Asymptotic D/S state D/S	0.0265	0.0271±0.0008[b,e]
Neutron-proton low-energy scattering (scattering length a; effective range r):		
$^1S_0$: a_s (fm)	−23.7451	−23.748±0.010[f]
r_s (fm)	2.7041	2.75±0.05[f]
$^3S_1$: a_t (fm)	5.4359	5.424±0.004[f]
r_t (fm)	1.7652	1.759±0.005[f]

[a]There is no direct experimental access to P_D.
[b]The "experimental" value for A_S is model dependent. In general, for its derivation energy *in*dependence of the nuclear force is assumed which however is not true for this model.
[c]Reference 22.
[d]Reference 23.
[e]Reference 24.
[f]Reference 25.

tributions to the baryon propagators. This again shows that baryon dressing is mainly an off-shell effect.

IV. SUMMARY

This is the second paper dealing with the extension of the Bonn meson-exchange *NN* interaction above pion production threshold, which requires the inclusion of nucleon and delta-isobar self-energy diagrams. While in the first paper[4] we have outlined the basic principles of our renormalization procedure and studied the consequences of nucleon renormalization, we have concentrated here on the effects resulting from the dressing of the Δ isobar. It turned out that, like below pion threshold, the inclusion of ρ exchange and retardation effects in the transition potentials is crucial.

In order to really establish the range of validity of the meson-exchange picture we have, in contrast to other authors, strictly avoided the use of different parameter values for the same meson-baryon-baryon vertex at different places, i.e., each vertex (e.g., $\pi N\Delta$) has the same parameter values in the $NN\to N\Delta$ ($\Delta\Delta$) transition potentials and in the isobar self-energy diagram. Of course, this restricts very much the possibilities of fitting data. Nevertheless, a reasonable description of the empirical data, especially of their resonance structure, up to 1 GeV could be obtained. Thus, there is no indication of a dramatic breakdown of the meson exchange concept in this region, and there appears to be no need for introducing genuine quark effects at this stage.

So far, crossed meson exchange diagrams (which are present in Ref. 1) have not been considered. Because of unitarity arguments, their inclusion would require to introduce in addition the whole set of nucleon and isobar self-energy diagrams up to fourth order in the πNN coupling constant explicitly, and would therefore lead to an enormous complication. Corresponding studies are planned for the future.

ACKNOWLEDGMENTS

This work is based on a Ph.D. thesis submitted by one of the authors (Ch.E.) to the Mathematische Naturwissenschaftliche Fakultät der Rheinischen Friedrich-Wilhelms-Universität Bonn. It was supported in part by the Deutsche Forschungsgemeinschaft (Az Ho730/5-2).

APPENDIX A: MODEL FOR πN SCATTERING IN THE P_{33} CHANNEL

If we build up the πN scattering amplitude T in the 33 channel by iterating the delta-isobar self-energy diagram [Fig. 2(b)], we obtain, in terms of unrenormalized $\pi N\Delta$ vertices $W^0_{\alpha\beta k}$ and bare isobar energy $E^{\Delta,0}_\alpha$,

$$\begin{aligned}T_{\beta' k'\beta k}(z)&=\sum_\alpha \frac{W^{0*}_{\alpha\beta' k}W^0_{\alpha\beta k}}{z-E^{\Delta,0}_\alpha}+\sum_{\beta''k''\alpha}\frac{W^{0*}_{\alpha\beta' k'}W^0_{\alpha\beta'' k''}}{(z-E^{\Delta,0}_\alpha)(z-E_{\beta''}-\omega_{k''})}T_{\beta''k''\beta k}(z)\\ &=\sum_\alpha \frac{W^{0*}_{\alpha\beta' k'}W^0_{\alpha\beta k}}{z-E^{\Delta,0}_\alpha}\sum_{n=0}^{\infty}\left[\frac{h_\alpha(z)}{z-E^{\Delta,0}_\alpha}\right]^n\\ &=\sum_\alpha \frac{W^{0*}_{\alpha\beta' k'}W^0_{\alpha\beta k}}{z-E^{\Delta,0}_\alpha-\hat{h}_\alpha(z)}\ ,\end{aligned}\tag{A1}$$

where $\hat{h}_\alpha(z)$ is the delta mass operator:

$$\begin{aligned}\hat{h}^\Delta_\alpha(z)&\equiv\sum_{\beta''k''}\frac{|W^0_{\alpha\beta''k''}|^2}{z-E_{\beta''}-\omega_{k''}+i\epsilon}\\ &=P\sum_{\beta''k''}\frac{|W^0_{\alpha\beta''k''}|^2}{z-E_{\beta''}-\omega_{k''}}-i\pi\sum_{\beta''k''}|W^0_{\alpha\beta''k''}|^2\delta(z-E_{\beta''}-\omega_{k''})\\ &\equiv h^\Delta_\alpha(z)-i\tilde{h}^{\Delta,0}_\alpha(z)\ .\end{aligned}\tag{A2}$$

Note that we take the renormalization of the nucleon intermediate state into account by using its physical energy $E_{\beta''}$.

The shift of the delta resonance position from the bare energy $E^{\Delta,0}_\alpha$ to the physical (renormalized) energy E^Δ_α is given by $h^\Delta_\alpha(E^\Delta_\alpha)=E^\Delta_\alpha-E^{\Delta,0}_\alpha$. Consequently, the propagator in Eq. (A1) can be written as

$$z-E^{\Delta,0}_\alpha-\hat{h}^\Delta_\alpha(z)=z-E^\Delta_\alpha+h^\Delta_\alpha(E^\Delta_\alpha)-h^\Delta_\alpha(z)+i\tilde{h}^{\Delta,0}_\alpha(z)\ .\tag{A3}$$

Noting that

$$h^\Delta_\alpha(E^\Delta_\alpha)(-h^\Delta_\alpha(z)=(z-E^\Delta_\alpha)[Z^{2,\Delta}_\alpha(z)-1]\tag{A4}$$

with

$$Z^{2,\Delta}_\alpha(z)\equiv 1+P\sum_{\beta k}\frac{|W^0_{\alpha\beta k}|^2}{(z-E_\beta-\omega_k)(E^\Delta_\alpha-E_\beta-\omega_k)}\tag{A5}$$

and making use of the definition of the renormalized matrix element $W^{(\Delta N\pi)}_{\alpha\beta k}\equiv W^0_{\alpha\beta k}/Z^\Delta_\alpha(E^\Delta_\alpha)$, Eq. (A3) goes into

$$z-E^{\Delta,0}_\alpha-\hat{h}^\Delta_\alpha(z)=(z-E^\Delta_\alpha)Z^{2,\Delta}(z)+i\tilde{h}^\Delta_\alpha(z)Z^{2,\Delta}_\alpha(E^\Delta_\alpha)\tag{A6}$$

since

$$\tilde{h}_\alpha^{\Delta,0}(z)=Z_\alpha^{2,\Delta}(E_\alpha^\Delta)\tilde{h}_\alpha^\Delta(z) \tag{A7}$$

with

$$\tilde{h}_\alpha^\Delta(z)\equiv\pi\sum_{\beta k}|W_{\alpha\beta k}^{(\Delta N\pi)}|^2\delta(z-E_\beta-\omega_k)\ . \tag{A8}$$

Furthermore, defining a dressing factor $r_\alpha^2(z)$ as

$$r_\alpha^2(z)\equiv\frac{Z_\alpha^{2,\Delta}(E_\alpha^\Delta)}{Z_\alpha^{2,\Delta}(z)} \tag{A9}$$

and

$$\Delta_\alpha(z)\equiv\tilde{h}_\alpha^\Delta(z)r_\alpha^2(z) \tag{A10}$$

the propagator can ultimately be written as

$$z-E_\alpha^{\Delta,0}-h_\alpha^\Delta(z)$$
$$=Z_\alpha^{2,\Delta}(E_\alpha^\Delta)\{z-[E_\alpha^\Delta-i\Delta_\alpha(z)]\}r_\alpha^{-2}(z)\ . \tag{A11}$$

So the T matrix Eq. (A1) can be written in terms of renormalized quantities only

$$T_{\beta'k'\beta k}(z)=\sum_\alpha\frac{W_{\alpha\beta'k'}^{*(\Delta N\pi)}W_{\alpha\beta k}^{(\Delta N\pi)}}{z-E_\alpha^\Delta+i\Delta_\alpha(z)}r_\alpha^2(z)\ . \tag{A12}$$

Explicitly $r_\alpha^{-2}(z)$ is given by

$$r_\alpha^{-2}(z)=1-(z-E_\alpha^\Delta)\sum_{\beta k}\frac{|W_{\alpha\beta k}^{(\Delta N\pi)}|^2}{(E_\alpha^\Delta-E_\beta-\omega_k)^2(z-E_\beta-\omega_k)}\ . \tag{A13}$$

Obviously, for $z=E_\alpha^\Delta$, $r_\alpha^{-2}(z)=1$ and the residue of the real part of the T matrix is given by the renormalized matrix elements $W_{\alpha\beta k}^{(\Delta N\pi)}$. Note, finally, that the Z factor, Eq. (A5), can also be written in terms of renormalized quantities, namely

$$Z_\alpha^{2,\Delta}(z)=1-P\sum_{\beta k}\frac{|W^{(\Delta N\pi)}|^2}{(z-E_\beta-\omega_k)(E_\alpha^\Delta-E_\beta-\omega_k)}\ . \tag{A14}$$

APPENDIX B: EVALUATION OF h_α^Δ, $\tilde{h}_\alpha^\Delta$, $Z_\Delta^{-2,\Delta}$, ${}_{N\Delta}R_{\alpha_1\alpha_2}^{-2}$, ${}_{\Delta\Delta}R_{\alpha_1\alpha_2}^{-2}$

Here, we evaluate explicitly the Δ-energy shift [Eqs. (A2) and (A8)], the Z factor [Eq. (A5)] and the $N\Delta$ [Eq. (2.5)], respectively, $\Delta\Delta$ dressing factor [Eq. (2.10)], based on the self-energy diagram, Fig. 2(b).

Starting point is the $\pi N\Delta$ (renormalized) interaction matrix element

$$W_{\alpha'\alpha n}^{(\Delta N\pi)}=-\frac{f_{N\Delta\pi}}{m_\pi}\frac{1}{[2\omega_{q-k}^\pi(2\pi)^3]^{1/2}}i(q-k)_\mu$$
$$\times\bar{u}^\mu(\mathbf{q},\lambda_{\alpha'})u(\mathbf{k},\lambda_\alpha)\cdot F_{\pi N\Delta}[(\mathbf{q}-\mathbf{k})^2]\ , \tag{B1}$$

where $u(\mathbf{k},\lambda_\alpha)$ denotes the usual (positive-energy) Dirac spinor with $u^+u=1$ and $\omega_{q-k}^{(\pi)}\equiv[m_\pi^2+(\mathbf{q}-\mathbf{k})^2]^{1/2}$ is the relativistic pion energy. $u^\mu(\mathbf{q},\lambda_{\alpha'})(\lambda_{\alpha'}=\pm\frac{3}{2},\ \pm\frac{1}{2})$ is the Rarita- Schwinger spinor describing the Δ isobar

$$u^\mu(\mathbf{q},\lambda)=\sum_{\substack{r,s\\ r+s=\lambda}}S_{s,\lambda}^\mu(\mathbf{q},r)u(\mathbf{q},s)\ , \tag{B2}$$

where $S_{s,\lambda}^\mu(\mathbf{q},r)$ is the spin-transition operator

$$S_{s,\lambda}^\mu(\mathbf{q},r)\equiv\sum_r\langle\tfrac{3}{2}\lambda\,|\,1r\tfrac{1}{2}s\rangle\varepsilon^\mu(\mathbf{q},r) \tag{B3}$$

$\varepsilon^\mu(\mathbf{q},r)$ $(r=1,2,3)$ are the polarization vectors fulfilling the completeness relation

$$\sum_{r=1}^3\varepsilon^\mu(\mathbf{q},r)\varepsilon^\nu(\mathbf{q},r)=-g^{\mu\nu}+\frac{q^\mu q^\nu}{m_\Delta^2} \tag{B4}$$

$F_{\pi N\Delta}$ is the $\pi N\Delta$ form factor, conventionally parametrized as

$$F_{N\Delta\pi}=\frac{\Lambda_{N\Delta\pi}^2-m_\pi^2}{\Lambda_{\pi N\Delta}^2+(\mathbf{q}-\mathbf{k})^2} \tag{B5}$$

$\Lambda_{\pi N\Delta}$ being the corresponding cutoff mass. [Note that the isospin dependence is suppressed in Eq. (B1).]

We first calculate $B_\lambda(\mathbf{q})\equiv\sum_{\alpha'k'}W_{\alpha\alpha'k'}^{(\Delta N\pi)}W_{\alpha'\alpha k'}^{(N\Delta\pi)}$, which appears in all quantities to be considered:

$$B_\lambda(\mathbf{q})=\frac{f_{N\Delta\pi}^2}{(2\pi)^3m_\pi^2}\int d^3k\frac{1}{2\omega_{q-k}^\pi}(q-k)_\mu\bar{u}^\mu(\mathbf{q},\lambda)\Lambda_+(\mathbf{k})u^\nu(\mathbf{q},\lambda)(q-k)_\nu F_{N\Delta\pi}^2\ . \tag{B6}$$

(The isospin dependence leads to a trivial factor of 1.)

If we put $\mathbf{q}$ into the z axis and $\mathbf{k}$ into the x-z plane, the polarization vectors are explicitly given by

$$\varepsilon^\mu(\mathbf{q},\pm1)=\frac{1}{(2)^{1/2}}\begin{pmatrix}0\\ \mp1\\ -i\\ 0\end{pmatrix};\quad \varepsilon^\mu(\mathbf{q},0)=\frac{1}{m_\Delta}\begin{pmatrix}q\\ 0\\ 0\\ E_q^\Delta\end{pmatrix} \tag{B7}$$

and Eq. (B6) goes into

$$B_\lambda(\mathbf{q})=\frac{f_{N\Delta\pi}^2}{(2\pi)^3m_\pi^2}\int d^3k\frac{1}{2\omega_{q-k}^\pi}\frac{E_q^\Delta E_k-\mathbf{q}\cdot\mathbf{k}+m_\Delta m}{2E_q^\Delta E_k}g_\lambda(q,k,\cos\theta)\cdot F_{N\Delta\pi}^2\ , \tag{B8}$$

where θ is the angle between $\mathbf{q}$ and $\mathbf{k}$ and

$$g_\lambda(\mathbf{q},k,\cos\theta)\equiv \sum_{s=-1/2}^{1/2}(q-k)_\mu S^{\mu *}_{s,\lambda}S^{\nu}_{s,\lambda}(q-k)_\nu \;. \tag{B9}$$

Specifically,

$$\begin{aligned} g_{3/2}&=\tfrac{1}{2}k^2(1-\cos^2\theta)\\ g_{1/2}&=\tfrac{1}{6}k^2(1-\cos^2\theta)+\tfrac{2}{3}\left[\frac{E_q^\Delta}{m_\Delta}\right]^2(q-k\cos\theta)^2 \end{aligned} \tag{B10}$$

which implies that the results will depend on the spin component of the Δ isobar.

Therefore we obtain for the energy shift

$$\frac{h^\Delta_{q,\lambda}(E_q^\Delta)}{Z^{2,\Delta}_{q,\lambda}(E_q^\Delta)}=\frac{f^2_{N\Delta\pi}}{(4\pi)^2m_\pi^2E_q^\Delta}\int_0^\infty dk\frac{k^2}{E_k}\int_{-1}^{+1}d\cos\theta\frac{(E_q^\Delta E_k+mm_\Delta-qk\cos\theta)g_\lambda(q,k,\cos\theta)F^2_{N\Delta\pi}}{\omega^\pi_{q-k}(E_q^\Delta-E_k-\omega^\pi_{q-k})} \tag{B11}$$

and

$$\begin{aligned}\tilde{h}^{\Delta}_{q,\lambda}(z-E_q)=\pi\frac{f^2_{N\Delta\pi}}{(4\pi)^2m_\pi^2E_q^\Delta}\int_0^\infty dk\frac{k^2}{E_k}\int_{-1}^{+1}d\cos\theta(E_q^\Delta E_k+mm_\Delta-qk\cos\theta)\\ \times g_\lambda(q,k,\cos\theta)F^2_{N\Delta\pi}(\omega^\pi_{q-k})^{-1}\delta(z-E_q-E_k-\omega^\pi_{q-k})\end{aligned} \tag{B12}$$

Furthermore,

$$\begin{aligned} Z^{-2,\Delta}_{q,\lambda}(E_q^\Delta)&=1-I^\Delta_{q,\lambda}\\ I^\Delta_{q,\lambda}&\equiv\frac{f^2_{N\Delta\pi}}{(4\pi)^2m_\pi^2E_q^\Delta}\int_0^\infty dk\frac{k^2}{E_k}\int_{-1}^{+1}d\cos\theta\frac{(E_q^\Delta E_k+mm_\Delta-qk\cos\theta)g_\lambda(q,k,\cos\theta)F^2_{N\Delta\pi}}{\omega^\pi_{q-k}(E_q^\Delta-E_k-\omega^\pi_{q-k})^2}\end{aligned} \tag{B13}$$

and the dressing factors become

$${}_{N\Delta}R^{-2}_{q,\lambda}(z)=1-(z-E_q-E_q^\Delta)[\Gamma^\Delta_{q,\lambda}(z-E_q)+\Gamma_q(z-E_q^\Delta)] \tag{B14}$$

with

$$\Gamma_q(z-E_q^\Delta)=\frac{g_\pi^2}{4\pi}\frac{\tau^2}{4\pi E_q}\int_0^\infty dk\frac{k^2}{E_k}\int_{-1}^{+1}d\cos\theta\frac{(E_qE_k-m^2-qk\cos\theta)F^2_{NN\pi}}{\omega^\pi_{q-k}(E_q-E_k-\omega^\pi_{q-k})^2(z-E_q^\Delta-E_k-\omega^\pi_{q-k})} \tag{B15}$$

for the nucleon dressing (see I) and

$$\Gamma^\Delta_{q,\lambda}(z-E_q)=\frac{f^2_{N\Delta\pi}}{(4\pi)^2m_\pi^2E_q^\Delta}\int_0^\infty dk\frac{k^2}{E_k}\int_{-1}^{+1}d\cos\theta\frac{(E_q^\Delta E_k+mm_\Delta-qk\cos\theta)g_\lambda(q,k,\cos\theta)F^2_{N\Delta\pi}}{\omega^\pi_{q-k}(E_q^\Delta-E_k-\omega^\pi_{q-k})^2(z-E_q-E_k-\omega^\pi_{q-k})} \tag{B16}$$

for the dressing of the Δ isobar. Finally,

$${}_{\Delta\Delta}R_q^{-2}(z)=1-(z-2E_q^\Delta)[\Gamma^\Delta_{q,\lambda_1}(z-E_q^\Delta)+\Gamma^\Delta_{q,\lambda_2}(z-E_q^\Delta)] \;. \tag{B17}$$

For $q=0$, the above expressions simplify considerably. Especially, the dependence on the spin component λ disappears since

$$\int_{-1}^{+1}d\cos\theta g_{1/2}(0,k,\cos\theta)=\int_{-1}^{+1}d\cos\theta g_{3/2}(0,k,\cos\theta) \;. \tag{B18}$$

For example, one obtains for the shift of the Δ-resonance position

$$\left.\frac{h_q^\Delta(E_q^\Delta)}{Z_q^{2,\Delta}(E_q^\Delta)}\right|_{q=0}=\frac{f^2_{N\Delta\pi}}{4\pi\cdot 6\pi m_\pi^2}\int_0^\infty dk\frac{k^4(E_k+m)}{E_k\omega_k^\pi(m_\Delta-E_k-\omega_k^\pi)} \tag{B19}$$

which is a well-known result from pion-nucleon scattering. In order to simplify the singularity structure and to get rid of the spin dependence in the dressing factors also for $q\neq 0$, the following approximate expression is used for Γ^Δ:

$$\bar{\Gamma}^\Delta_q(z-E_q)=\frac{f^2_{N\Delta\pi}}{4\pi\cdot 6\pi m_\pi^2E_q^\Delta}\int_0^\infty dk\frac{k^4m_\Delta(E_k+m)F^2_{N\Delta\pi}}{E_k(m_\Delta-E_k-\omega_k^\pi)^2(z-E_q-E_k-\omega^\pi_{qk})\omega_k^\pi} \;. \tag{B20}$$

This form keeps the important threshold behavior and ensures that $\bar{\Gamma}^\Delta$ still vanishes for sufficiently large q. [$\omega^\pi_{qk}\equiv(m_\pi^2+q^2+k^2)^{1/2}$, which is obtained by putting $\cos\theta=0$.] An analogous expression is taken for the dressing factor $\bar{\Gamma}^\Delta_q(z-E_q^\Delta)$ appearing in the $\Delta\Delta$-box diagrams. For further details we refer the reader to Ref. 21.

*Present address: Department of Physics, Kent State University, Kent, OH 44242.
†Also at Institut für Kernphysik der KFA Jülich, D-5170 Jülich, Federal Republic of Germany.

[1]R. Machleidt, K. Holinde, and Ch. Elster, Phys. Rep. **149**, 1 (1987).
[2]R. A. Arndt *et al.*, Phys. Rev. D **28**, 97 (1983).
[3]R. Dubois *et al.*, Nucl. Phys. **A377**, 554 (1982).
[4]Ch. Elster, W. Ferchländer, K. Holinde, D. Schütte, and R. Machleidt, Phys. Rev. C **37**, 1647 (1988).
[5]K. Holinde and R. Machleidt, Nucl. Phys. **A280**, 429 (1977); K. Holinde, R. Machleidt, M. R. Anastasio, A. Faessler, and H. Müther, Phys. Rev. C **18**, 870 (1978).
[6]R. A. Arndt, interactive dial-in program SAID.
[7]W. M. Kloet and J. A. Tjon, Phys. Rev. C **30**, 1653 (1984).
[8]E. van Faassen and J. A. Tjon, Phys. Rev. C **33**, 2105 (1986).
[9]F. Shimizu *et al.*, Nucl. Phys. **A386**, 571 (1982).
[10]W. M. Kloet and R. R. Silbar, Nucl. Phys. **A364**, 364 (1981).
[11]W. Jauch, A. König, and P. Kroll, Phys. Lett. **143B**, 509 (1984).
[12]E. Aprile-Giboni *et al.*, Nucl. Phys. **A431**, 637 (1984).
[13]R. Hess, Proceedings of the 6th International Symposium on High Energy Spin Physics, Marseille, 1984, edited by J. Soffer [J. Phys. (Paris) Colloq. **46**, C2 (1985)].
[14]J. P. Stanley *et al.*, Nucl. Phys. **A403**, 525 (1983).
[15]I. P. Auer, LA-UR-83-36/2, 1983 Los Alamos Meson Physics Facility Report.
[16]I. P. Auer, Phys. Rev. Lett. **41**, 354 (1978).
[17]P. U. Sauer, in *Progress in Particle and Nuclear Physics* (Pergamon, Oxford, 1985), Vol. 16, p. 35.
[18]T.-S. H. Lee and A. Matsuyama, Argonne Report PHY-4863-TH-86, 1986; T.-S. H. Lee, Phys. Rev. C **29**, 195 (1983).
[19]G. Höhler, F. Kaiser, R. Koch, and E. Pietarineu, Handbook of Pion Nucleon Scattering, Fachinformationszentrum Energie, Physik, Mathematik GmbH Karlsruhe, Report 12-1, 1979.
[20]W. Ferchländer, D. Hirt, and D. Schütte (unpublished).
[21]Ch. Elster, Ph.D. thesis, University of Bonn, 1986.
[22]C. van der Leun and C. Alderliesten, Nucl. Phys. **A380**, 261 (1982).
[23]D. M. Bishop and L. M. Cheung, Phys. Rev. A **20**, 381 (1979).
[24]T. E. O. Ericson and M. Rosa-Clot, Nucl. Phys. **405**, 497 (1983); T. E. O. Ericson, *ibid.* **A416**, 281c (1984).
[25]O. Dumbrajs *et al.*, Nucl. Phys. **B216**, 277 (1983).
[26]J. Bystricky, C. Lechanoine-Leluc, and F. Lehar, J. Phys. (Paris) **48**, 199 (1987).
[27]F. Lehar, C. Lechanoine-Leluc, and J. Bystricky, J. Phys. (Paris) **48**, 1273 (1987).